Journal of Ubiquitous Computing and Communication Technologies (ISSN: 2582-337X)
www.irojournals.com/jucct/

Performance Analysis of Isolated Bridgeless SEPIC Converter for EV Battery Charging

K. Vinothini[1], P. Maruthupandi[2]

[1,2]Department of Electrical and Electronics Engineering, Government College Of Technology, Anna University, Coimbatore, Tamil Nadu, India

E-mail: [1]vinothini4777@gmail.com, [2]pandi@gct.ac.in

Abstract

The conventional Electric Vehicle(EV) battery charging systems with power factor correction circuits have limitations due to conduction losses present in the input side bridge rectifiers. This paper presents a Bridgeless Isolated Single-Ended Primary Inductance Converter (SEPIC) with improved power factor and reduced THD to increase performance. Throughout the charging time of the Electrical Vehicle, the input side maintains a near-unity power factor. Because the DBR is eliminated, the current is conducted through a smaller number of devices, resulting in considerable reductions in conduction losses. This optimizes the charging system's efficiency in alternative to the existing BL SEPIC converter. A constant current/constant voltage controlling mode is used to charge the EV battery, which delivers good results in terms of intrinsic PFC and decreased THD, hence increasing the charging performance of this system.

Keywords: Bridgeless Isolated SEPIC converter; CC/CV mode; Total Harmonic Distortion (THD); Discontinuous conduction mode (DCM)

1. Introduction

The automobile sector is turning to electric vehicles to reduce greenhouse gas emissions. Energy storage known as BES (Battery Energy Storage) is a contemporary and forthcoming electric-vehicle technology in which charging integrates specific power electronic interface circuits as explained in [1-3]. The standard EV battery charging method is powered by a diode bridge rectifier's filtered output, which is powered by an AC supply (DBR). This sort of charging method uses AC mains to extract a highly distorted current. As a result, losses in the traditional system grow. In the market for charging systems, stage with only one stage power factor correction converters are being studied extensively [3]. The full-

DOI: https://doi.org/10.36548/jucct.2022.1.004
Received: 11.03.2022, received in revised form: 16.04.2022, accepted: 30.04.2022, published: 09.05.2022

bridge architecture looks to be a solution for systems. The additional components in the four driving circuits adds to the complexity. [4]. Low Electromagnetic Interference noise, greater power density, and excellent efficiency across a input side voltage are all advantages in an LLC resonant converter based on charging system [5].

The increasing and decreasing features of a large range of input side voltages in buck-boost converters [6] are a viable alternative for PF correction in EV charging. As a result, electric vehicles require a specialized converter architecture. [7] discusses a complete examination of the numerous single-phase AC-DC buck-boost power factor correction converters, including their setups and performance testing in various operating conditions.

There is a circuit for a standard PFC SEPIC converter [8] with a bridgeless layout in the literature. Gabri et al. explained a newly designed SEPIC converter which having good gain and efficiency in [9]. However, the additional number of components required to widen the gain range increases the converter's cost and size.

Sabzali et al. [10] demonstrated the functioning of three BL SEPIC converters with low current ripple and ease of implementation. Furthermore, because the intermediate capacitors are coupled in topology-1 [11], the problem of circulation losses is severe. A new approach to power factor adjustment. To tackle the problem of circulating current, the SEPIC circuit is invented in [12]. However, the converter also having the disadvantage of a lower power density, no isolation between input and output.

This paper proposes the implementation and design of a novel bridgeless isolated SEPIC converter. The aims of nearly unity power factor and reduced THD are achieved. The advantages of the proposed system, are as follows.

A common input inductor replaces the bridge rectifier at the supply side of traditional BL converters. Due to comparable gate pulses supplied to both switches, the converter's pulse pattern is simpler.

The SEPIC BL converter's magnetizing inductance is designed in DCM, resulting in a further decrease in the size and cost of the charging system and it improves efficiency of the converter.

Simulation results for the proposed system using a MATLAB/Simulink, under steady-state for the entire charging duration are discussed.

2. Proposed Electric Vehicle Battery Charging System

The bridgeless isolated SEPIC converter takes the AC supply as an input and it is given to the battery for charging application**.** Figure 1 shows the block diagram of system.

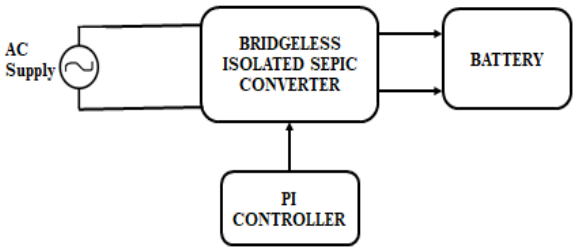

Figure 1. Block diagram of the System

A cascaded dual PI controller helps to maintain the current of the battery while the constant current and voltage control mode. A precise reference value, such as a continuous current flowing through the battery. The SEPIC converter uses a discontinuous conduction mode, which has several advantages, including sharing the input side inductor across the two halves and removing the electromagnetic interference LC filter.

2.1 Operation Analysis

The proposed EV charging system has two separate SEPIC power factor correction converters that work in the power supply's alternating cycles, which can be seen in Figure 2. Conduction loss associated with switching devices is decreased by eliminating an input DBR and replacing it with a common input inductor**.**

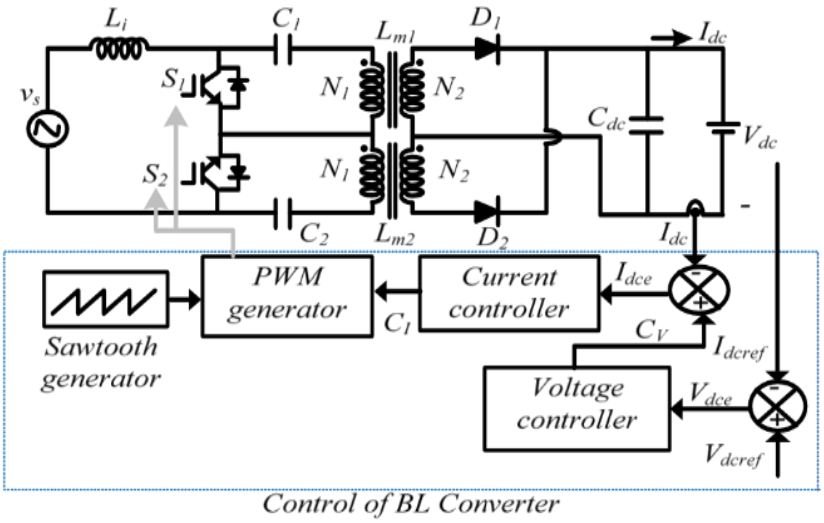

Figure 2. Circuit Diagram of Isolated Bridgeless SEPIC Converter

The working of the two PI controllers is consistent to provide a speed dynamic response loop and minimal error of the steady state. During constant current/constant voltage control charging, a cascaded dual PI controller manages the battery current. The gate signals, which are produced simultaneously using the PWM control approach, are used to drive the PFC switches. The enhanced charging of the battery is illustrated with the results of the simulation to design converter's working operation under various operating situations. The isolated BL topology has two switches that function separately. As in Figure 2, the BL circuit works in six distinct modes. (c)-(h), respectively, for positive half-cycle.

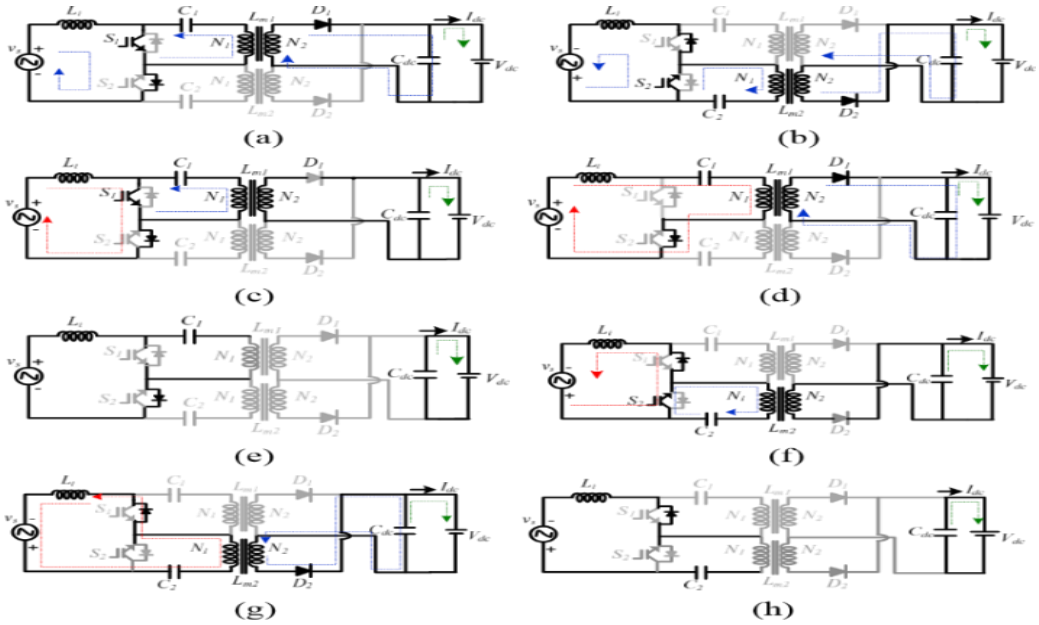

Figure 3. Operating principle (a)-(b) Positive and negative half-cycle operation, as well as operating during a single switching cycle

Mode-1: When the switch S1 in ON state, then, a current flow through the input side inductance Li linearly rises. As seen in Figure 2, the primary side capacitor, C1, releases while the magnetizing inductor, Lm1, retains the stored energy (c).

$$i_{Li}(t)=I_{Li}(t_0)+\frac{V_{in}}{L_i}(t\text{-}t_0)\ For\ t_0\leq t\leq DT_s \tag{1}$$

$$i_{Lm1}(t)=I_{Lm1}(t_0)+\frac{V_{C1}}{L_{m1}}(t\text{-}t_0) \tag{2}$$

The symbol D is the needed duty cycle for a converter with a transformation ratio of (N1/N2) to keep the output voltage 48V at all times. The switching time is Ts, the rated

mains voltage is Vin, and the current via the magnetizing inductance is iLm1. Now, using the formula, the current via the switch of the converter is estimated by equation (3)

$$i_{s1}(t)=I_{Li}(t_0)+I_{Lm1}(t_0)+\frac{V_{in}}{L_i /\!/ L_{m1}}DT_s \tag{3}$$

Mode-2: When the switch S1 is switched off, the current flow in the two inductor currents, iLi and iLm1, causes the output diode D1 to conduct. As a consequence, the rate of inductor currents iLi and iLm1 seems to be decreasing. During this mode,

$$V_{in}(t)D+\left(V_{in}(t)\text{-}V_{C1}\text{-}nV_{dc}\right)D_1=0 \tag{4}$$

where D1 is the time the converter is in DCM mode, and Vc1 is the voltage throughout the intermediate capacitor C1 while it is flowing in half of the cycle. The inductor current is expressed as an equation (5).

$$i_{L_{m1}}(t)=I_{L_{m1}}(t_0)+\frac{V_{in}}{L_{m_1}}DT_s+\frac{V_{in}\text{-}V_{C1}\text{-}nV_{dc}}{L_{m_1}}\left(t\text{-}t_1\right) \tag{5}$$

Mode-3: The switch S1 is in the OFF state, and the energy which is stored in the high frequency transformer primary side inductance Lm1 has been discharged. The inductor current and switch current expressions are presented as an equation (6)

$$I_{Li}(t)=I_{Li}(t_0)+\frac{V_{in}}{L_i}DT_s+\frac{V_{in}\text{-}V_{C1}}{L_i}\left(t\text{-}t_2\right) \tag{6}$$

In SEPIC mode, the negative half cycle of the voltage, a similar series of operations is observed.

3. Design of the Proposed System

Input supply voltage (Vs) = 220V, Frequency (f) = 50 Hz, HFT transformation ratio (N_1:N_2) =1.305, inductor ripple current L_i (ΔiL_i)= 20% of I_i, ripple voltage in capacitor C1 (ΔVc1) = 20% of average supply voltage , switching frequency = 10kHz. The battery used is a lead-acid battery with 48V and 100Ah capacity. The input supply voltage of the converter, V_s is estimated by an equation (7).

$$V_{sav}=\frac{2\sqrt{2}xV_s}{\pi} \tag{7}$$

The converter duty cycle is set at 0.3, resulting in a DC output voltage of 48 volts. The HFT transformation ratio N1/N2 is 1.305 when all the design values in the preceding formula are substituted. For a significant ripple current specified by Δi_i, the value of input inductance is calculated as follows,

$$L_i=\frac{V_sD}{2fs\Delta i1}=4.3Mh \tag{8}$$

For this application, the switching frequency given is 10 KHz. The following equations must be evaluated to achieve an adequate amount of high-frequency transformer magnetizing inductance.

$$R_{dc}=\frac{V_{dc}{}^2}{P_{out}}=5.81\ \Omega \tag{9}$$

In addition, the inductance of the high frequency transformer is calculated as equation (10) to maintain the magnetizing inductor during the switching cycle,

$$L_{mc}=\left(\frac{N1}{N2}\right)^2\ \frac{V_{dc}(1-D^2)}{2Df_sI_{dc}}=227\mu H \tag{10}$$

As a result, the chosen magnetizing inductance value is smaller than that calculated, i.e. 100H, resulting in enhanced PQ-based converter functioning at all operating voltages. The choice of energy transfers capacitors C1 and C2 have a direct impact on the proposed charger's wave-shaping capability.

$$C_{1,2}=\frac{N2}{N1}\ \frac{V_{dc}\ D}{(\Delta V_{C1,2}\ \ f_s\ R_{dc})}=5.6\mu F \tag{11}$$

Therefore, 5.6μF capacitance is chosen in this work, to operate the primary side capacitors C_1 and C_2 in CCM. For a 10% ripple in output voltage, the DC-link capacitor to provide rated battery load is calculated as,

$$C_{dc}=\frac{I_{dc}}{(2\omega\Delta V_{dc})}=2.86mF \tag{12}$$

As a result, a 2.86mF capacitor is used to keep the charging signals at predetermined limits, extending for battery's life.

3.1 Control Strategy

A PI controller with the dual loop is employed for the proposed charging method to ensure optimal charging of the EV battery. Two switches operate in synchronism for each cycle of the supply voltage. As a result of using the identical gating signals for two switches,

the controlling implementation is simple and clear. The control circuitry uses a voltage PI controller to achieve a CC/CV charging technique for an EV battery charging system, in which the voltage level of the battery, Vdc, is regulated. The current PI controller is used to keep the charging current, Idc, within limitations. At every sampling instant, the error is minimized by k, the aforementioned voltage error, and the control signal.

The K_{pv} and K_{iv} represent the proportional gain constant and integral gain constant, respectively use for voltage control. The desired reference is generated by the regulated voltage output Cv from this PI controller for managing current. With KpI and KiI for the current loop, k is the sampling instant. A PWM control solution generates the required gate pulses for the converters by comparing the output value of the current PI controller to a sawtooth wave of 10 kHz. The control changes to CV mode after reaching an 80 percent state of charge.

4. Simulation Results and Discussions

The improved EV battery charging system is validated using MATLAB/Simulink. Simulation results with battery load for open loop and closed loop are discussed.

4.1 Open-loop bridgeless Isolated SEPIC Converter

The open-loop bridgeless isolated SEPIC converter has simulated and it is shown in Figure 4.

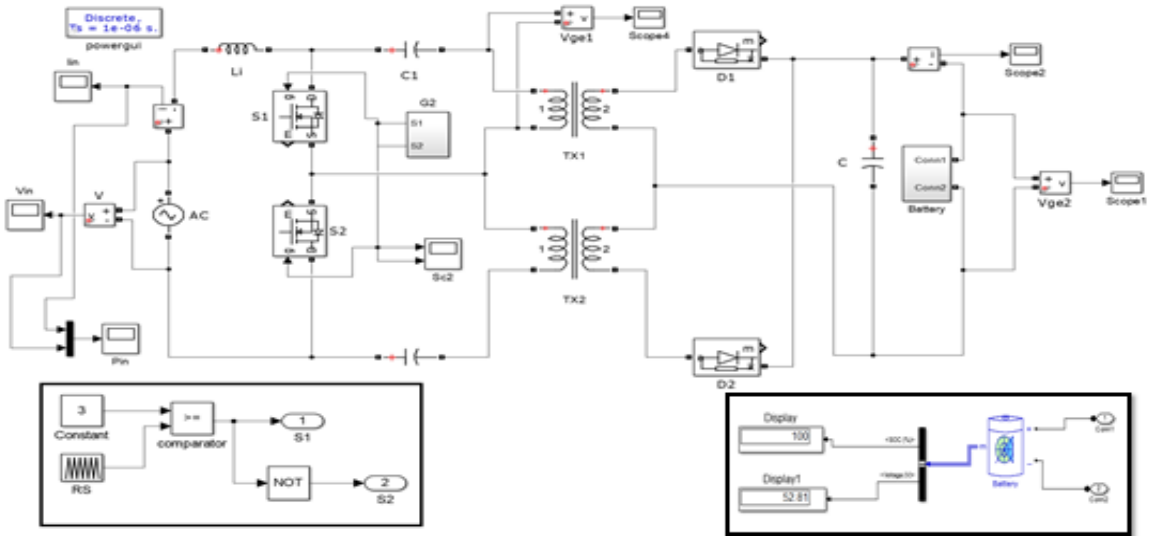

Figure 4. Open-loop BL isolated SEPIC converter simulation diagram.

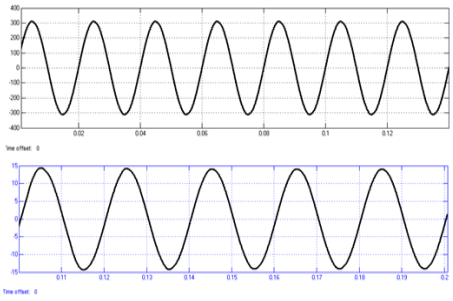

Figure 5. Supply Voltage and supply current waveform

The bridgeless isolated SEPIC converter in an open loop is performed with supply voltage of 220V AC supply with duty cycle D=0.3. PWM control methods are used to drive the PFC switches using gate signals. Figure 5 depicts the input current 15A, which is measured in charging mode for an open-loop bridgeless isolated SEPIC converter.

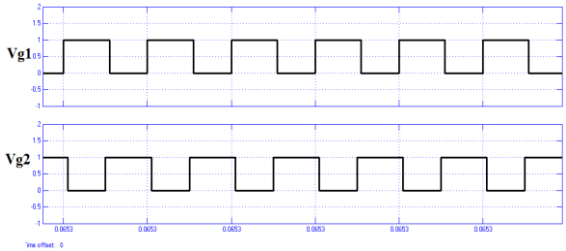

Figure 6. Switching pulse waveform

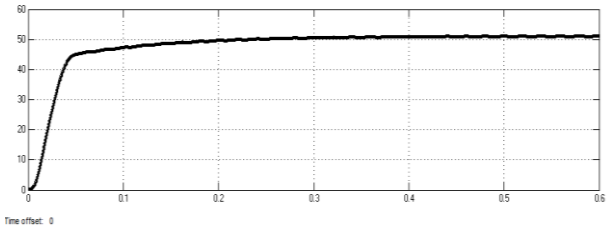

Figure 7. output voltage waveform

Independent and individual activation of switch S1 and switch S2 throughout the corresponding half cycle confirms the converter's bridgeless operation. Figure 6 shows an obtained pulse pattern wave form of the converter.

4.2 Closed-loop BL Isolated SEPIC converter

The closed-loop bridgeless isolated SEPIC converter by using the control strategy for PI controller is simulated. The converter is performed with the input voltage of 220V AC supply with duty cycle D=0.3.

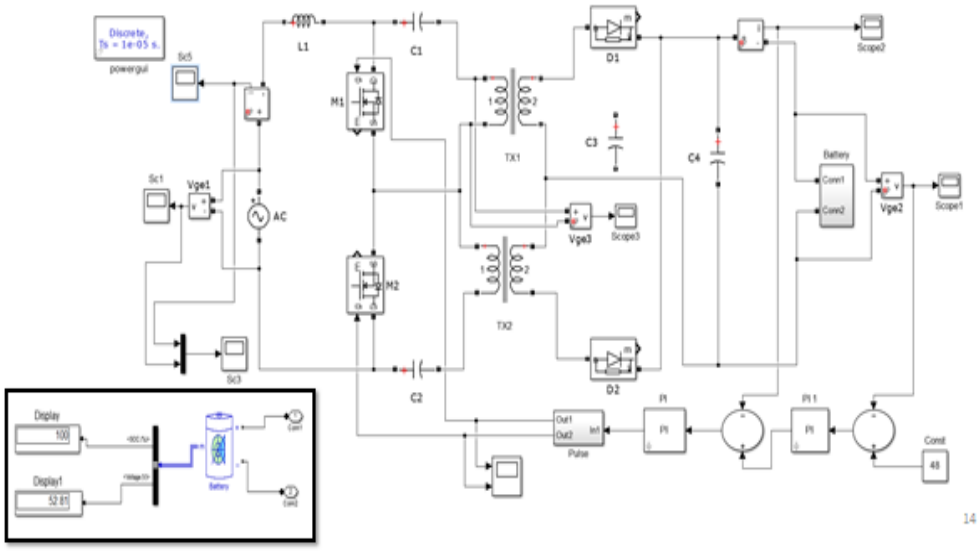

Figure 8. Closed-loop BL isolated SEPIC Converter with PI controller simulation diagram

The needed gate pulses for the PI controller's converter is 10 kHz are generated using a PWM control approach. As a result, to give gate signals to switch S1 and switch S2, an adaptable duty cycle is provided. A sinusoidal current is obtained from the source in phase with the AC supply voltage, as shown in Figure 9. As a result, operation with a near-unity power factor is assured. For a closed-loop bridgeless isolated SEPIC converter, a rated current of the battery,15A was observed in charging mode.

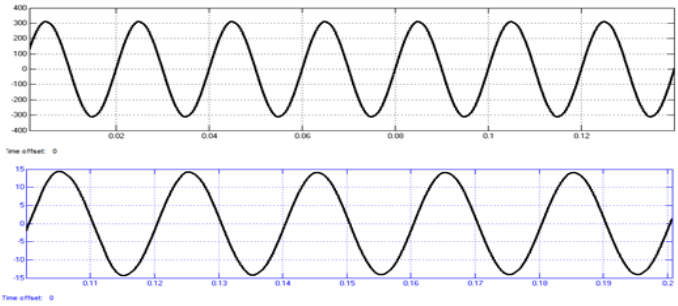

Figure 9. Supply voltage and supply current waveform

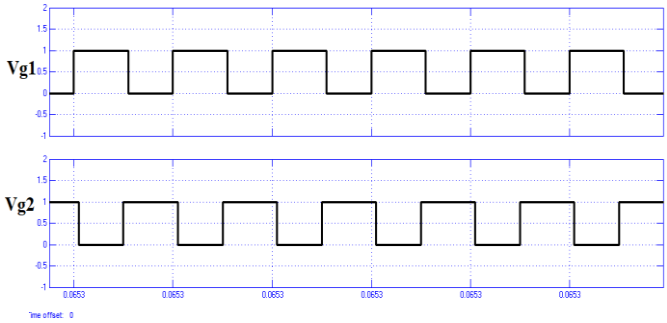

Figure 10. Switching pulse waveform

Figure 10 shows an obtained switching pulse waveform for a closed-loop bridgeless isolated SEPIC converter. Independent and individual activation of switch S1 and switch S2 throughout the corresponding half cycle confirms the converter's bridgeless operation.

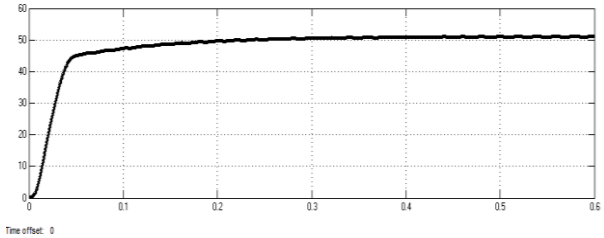

Figure 11. Output voltage Waveform

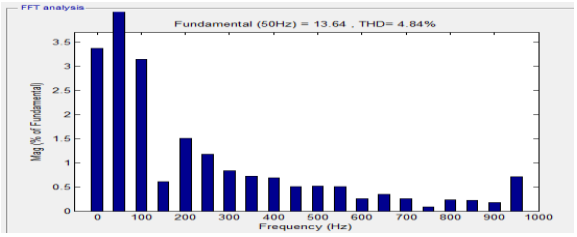

Figure 12. Supply current THD

Figure 11. Shows obtained output side voltage of the closed-loop bridgeless isolated SEPIC converter is 48V across battery load. Figure 12 shows that the supply current THD, which is 4.84% for closed loop system.

4.3 Comparison of Conventional Bridgeless Converters

Table 1 shows the comparison of the proposed charging mechanism to the traditional charging system. In the proposed work, the recorded mains current is in sinusoidal shape and power factor to unity also input current THD is noted as 4.8%.

Table 1. Comparison between proposed charging system and Conventional charging system

Elements	**BL Isolated PFC Converter charging system**	**Conventional PFC fed charging systems**
High-frequency device	Two	Two
Slow diode	None	Four
Fast recovery diode	Two	Two

Table 1 compares the proposed EV charging system to the traditional SEPIC power factor correction-based charging system in terms of the number of components. When compared to an existing PFC-based charger, it seems that the conduction of the current in the proposed system happens through the lesser components with a shared common inductor. This lowers the cost of the devices while also reducing the size of the charger and increasing overall efficiency.

5. Conclusion and Future work

The relevant design requirements in discontinuous conduction mode and control approach for enhancing the power factor close to unity have been proposed for a novel isolated BL SEPIC converter-based EV battery charging system. The availability of a common input inductor during both half cycles is a benefit of the proposed system. The input current is reconfigured in phase with supply voltage, and also the AC supply current THD is decreased to 4.8 percent, compared to typical EV chargers. In future work, the hardware design of the simulation work can be implemented**.**

References

[1] N. Mohan, T. M. Undeland, and W. P. Robbins, *Power Electronics: Converters, Applications, and Design*. Hoboken, USA: Wiley, 2009.

[2] SAE Electric Vehicle and Plug-in Hybrid Electric Vehicle Conductive Charge Coupler, SAE Std. J1772, 2010.

[3] S. Dusmez and A. Khaligh, "A compact and integrated multifunctional power electronic interface for plug-in electric vehicles," *IEEE Transactions Power Electronics*, vol. 28, no. 12, pp. 5690-5701, Dec. 2013.

[4] H. Vu and W. Choi, "A Novel Dual Full-Bridge LLC Resonant Converter for CC and CV Charges of Batteries for Electric Vehicles," *IEEE Transactions Industrial Electronics*, vol. 65, no. 3, pp. 2212-2225, March 2018.

[5] S. Jeong, J. Kwon, and B. Kwon, "High-Efficiency Bridgeless Single-Power-Conversion Battery Charger for Light Electric Vehicles," *IEEE Transactions Industrial Electronics*, vol. 66, no. 1, pp. 215-222, Jan. 2019.

[6] B. Zhao, A. Abramovitz, and K. Smedley, "Family of BL buck-boost PFC rectifiers," *IEEE Transactions Power Electronics*, vol. 30, no. 12, pp. 6524-6527, Dec. 2015.

[7] B. Singh, S. Singh, A. Chandra, and K. Al-Haddad, "Comprehensive study of single-phase AC-DC power factor corrected converters with high-frequency isolation", *IEEE Trans. Ind. Informatics*, vol. 7, no. 4, pp. 540-556, Nov. 2011.

[8] S. Durgadevi and M. G. Umamaheswari, "Analysis and design of single-phase power factor correction with DC-DC SEPIC Converter for a fast dynamic response using a genetic algorithm optimized PI controller," *IET Circuits, Devices & Systems*, vol. 12, no. 2, pp. 164-174, 2018.

[9] A. M. Al Gabri, A. A. Fardoun and E. H. Ismail, "Bridgeless PFC-modified SEPIC rectifier with extended gain for universal input voltage applications," *IEEE Transactions Power Electronics*, vol. 30, no. 8, pp. 4272-4282, Aug. 2015.

[10] A. J. Sabzali, E. H. Ismail, M. A. Al-Saffar and A. A. Fardoun, "New bridgeless DCM SEPIC and Cuk PFC rectifiers with a low conduction and switching losses," *IEEE Transactions Industry Applications*, vol. 47, no. 2, pp. 873-881, March-April 2011.

[11] H. Ma, Y. Li, J. Lai, C. Zheng, and J. Xu, "An improved bridgeless SEPIC converter without circulating losses and input-voltage sensing," *IEEE Journal of Emerging and Selected Topics in Power Electronics*, vol. 6, no. 3, pp. 14471455, Sept. 2018.

[12] Y. Wang, N. Qi, Y. Guan, C. Cecati and D. Xu, "A single-stage LED driver based on SEPIC and LLC circuits," *IEEE Trans. Ind. Elect.*, vol. 64, no. 7, pp. 5766-5776, July 2017.